

Contents

List of figures	II
List of tables	III
1 Introduction	1
1.1 Motivation	1
1.2 Troubles	1
1.3 Approach	2
2 Theory	3
3 Experimental	4
4 Analysis	5
4.1 Isotherm computation	5
4.1.1 Volumetric isotherm	5
4.1.1.1 Porosity	7
4.1.1.2 Determination of the saturated vapor pressure	8
4.1.1.3 Diameter error using Kelvin equation	8
4.1.2 Optical measurements	8
4.2 Conducted measurements	9
4.3 Inhomogeneities on one wafer	9
4.4 Comparison of closed and open pores	9
4.4.1 Bad open pores	9
4.4.2 Inverse funnelling	9
4.4.2.1 Immersion experiment	9
4.4.2.2 Inverse funnelling upon barrier layer dissolution	9
4.4.3 Etch rate difference	10
4.4.3.1 Pore opening widening pores much less than expected	10
4.4.3.2 Floating experiment	10
4.4.4 Do thinner membranes improve things?	10
4.5 Testing theory using electron beam microscopy	10
4.6 Pore size reduction using atomic layer deposition	10
4.7 Isotherms proves powerful to detect and characterize defects	10
Bibliography	11

List of Figures

- 4.1 Raw volumetric isotherm data recorded with the experimental setup as explained in ?? for one cycle without a membrane inside the cell and one with a membrane inside the cell. (a) shows the pressure values over time making the condensation and evaporation plateaus of absorption and desorption of hexane within the membrane's pores visible. (b) is the pressure loop which is relevant for the computation of the isotherms. Again, the before mentioned plateaus are visible as dips in the time derivative of the pressure. 6
- 4.2 (a) shows the raw data of the isotherm with membrane and interpolation of the reference isotherm without membrane. Also, the subtraction of the latter (compare integrand of eq. (4.1)) is plotted where the area to be integrated for the absorption and desorption isotherm is shaded light green. The integration according to eq. (4.3) results in the isotherm displayed in (b). 7

List of Tables

- 4.1 Wafer specifications. The wafers thickness l_{pore} , floating time t_{float} of the *barrier layer* dissolution process and pore diameter dispersion $\Delta d_{\text{pore}}^{\text{MEB}}$ measured by electron beam microscopy are noted. The latter two parameters apply to the open pore membranes of the respective wafer. 9

1 Introduction

1.1 Motivation

The fundamental idea is to test models of condensation and evaporation of liquids in confinement. To this end, a well characterized confinement is necessary. The latter shall be realized using nanoporous alumina membranes. The production of these is rather advanced as they are commonly used for the production of nanowires. Moreover, the shape of the pores is ideally cylindrical which makes for a simple geometry. A nanoporous alumina membrane includes a large number of parallel pores. Therefore, any experiment conducted on one of these membranes yields a result that averages over all of these pores. This is why, ideally, monodisperse alumina membranes shall be produced.

As a liquid to condense inside the pores of these membranes, hexane is used. There are multiple reasons for that. First, other teams have used hexane for this type of experiments before. This means that reference isotherms exist that the results can be compared to. Moreover, hexane permits to experiment at ambient temperature which makes things much easier. The fact that this is only a preexperiment for later experiments using helium, the use of liquids like nitrogen seems to make experimenting more difficult while offering no advantages.

The models to be tested are primarily the KELVIN equation and the SAAM and COLE theory. There are multiple variations though, as for example there is a modified KELVIN equation taking into account the wetting film which the basic KELVIN equation does not. In addition to that, thermal activation and the temperature relative to the critical temperature of the used fluid are relevant. The latter is one reason why finally, the experiment is planned to be conducted using helium. Finally, there are other more sophisticated models that need to be tested. Due to the small variations that are expected, again, the probing of the latter requires helium. Last but not least, in order to also study cavitation in alumina membranes, inc bottle like cavities with constricted openings must be produced. As for both, the helium experiments and for the inc bottle openings, pores of sub ten nanometer diameter must be synthesized in a controlled way, the production process needs to be improved. This becomes the main goal of the conducted experiments described in this article.

1.2 Troubles

Early on, the conducted experiments prove the membranes to be not as ideal as was hoped for. The idea of the perfect cylindrical pores of the same diameter is replaced by the conclusion that the pores' diameter is not only distributed over the membranes but also varies within a single pore. This variation manifests in the way of a funnelling aspect that makes for a conical shape, rather than a cylindrical, and also as corrugations. As explained above, the confinement needs to be well characterized to be able to test the models of condensation and evaporation. In contrast to that, the geometrical shape of the pores does not allow for this kind of precise characterization. Using electron beam microscopy, the opening diameters of the pores can be checked on top and bottom side. Furthermore, a cross section view yields some information about the straightness and possible defects along the length of the pores. As the pores' length ranges in the order of micrometers though, while the diameters' magnitude is nanometers, this still gives little information about the overall pore shape. Moreover, the microscopy images can not be precisely evaluated due to the unknown porosity of the membranes and again the lack of information on the shape. In the course of the experiments

a way is developed to at least delimit a range for the porosity and so allow for a more sophisticated analysis of the electron beam microscopy images under the assumption of a certain pore geometry.

The bottom line is that neither the exact geometry and distribution of pore shapes and sizes is known, nor are the condensation and evaporation models clear. Thus, the first step must be to understand and refine the production process of the membranes and to hereby make for the best possible characterization of the confinement.

1.3 Approach

To understand the membranes' characteristics and to use this knowledge to improve the production process, rather large pore diameters of above forty nanometer diameter, for which KELVIN equation is assumed to be sufficiently precise, are probed using multiple techniques. The core of the conducted experiments relies on thermodynamics using volumetric measurements. In addition, optical measurements and also visual documentation are used along with electron beam microscopy. All the aquired data is then interpreted and tested for coherence to finally draw conclusions on the membranes' characteristics. From the aquired results, questions rise about the effects of different production steps which are then taken a closer look at.

2 Theory

3 Experimental

4 Analysis

4.1 Isotherm computation

In the following, evaluation of the recorded raw data is presented for volumetric (section 4.1.1) and for the optical measurements (section 4.1.2).

4.1.1 Volumetric isotherm

To compute the isotherms from the recorded data the experiment needs to be conducted not only with a membrane inside of the cell, but also with an empty cell. From here on, the following indices shall be used:

- 1 \longrightarrow no membrane
- 2 \longrightarrow membrane.

Furthermore, the variables P_i , \dot{P}_i , V_i , T_i , n_i and \dot{n}_i , $i \in \{1, 2\}$, refer to the values measured inside of the cell, in explanation the red marked part of the system in ???. The raw isotherms of the two experiments are shown in fig. 4.1. The plateaus of the yellow curve with membrane inside the cell of the plot versus time correspond to the dips of the time derivative of the pressure of the versus pressure plot. This can be explained by the hexane condensing inside the membrane's pores at a given pressure due to which the continuing matter flow into the cell does not yield an increase of pressure.

Regarding the system with and empty cell, it is clear that the ideal gas law can be used to compute the flow rate of hexane (compare ???). By solving for the amount of matter

$$n_1 = \frac{P_1 V_1}{RT_1},$$

taking into account that the temperature of the cell is regulated at T_1 and the volume V_1 is constant, the flow of matter becomes

$$\dot{n}_1 = \frac{V_1}{RT_1} \cdot \dot{P}_1.$$

Furthermore, the flow of matter for the system with a membrane inside the cell can be interpreted as the sum of the flow into the membrane \dot{n}_2^{mem} and the flow into the system volume excluding the membrane \dot{n}_2^{cell} . This can be rewritten yielding

$$\dot{n}_2^{\text{mem}} = \dot{n}_2 - \dot{n}_2^{\text{cell}},$$

where \dot{n}_2^{cell} obeys ideal gas law. Using the fact that the flow through the PFEIFFER valve only depends on the pressure difference $\Delta P_i = P_i^{\text{tank}} - P_i^{\text{cell}}$, assuming that $P_1^{\text{tank}} = P_2^{\text{tank}}$ leads to

$$\begin{aligned} \dot{n}_2^{\text{mem}}(P_2) &= \dot{n}_1(P_2) - \dot{n}_2^{\text{cell}}(P_2) \\ &= \frac{V_1}{RT_1} \cdot \dot{P}_1(P_2) - \frac{V_2}{RT_2} \cdot \dot{P}_2(P_2) \end{aligned} \quad (4.1)$$

Figure 4.2(a) shows the computation steps visually using the respective plots versus time.

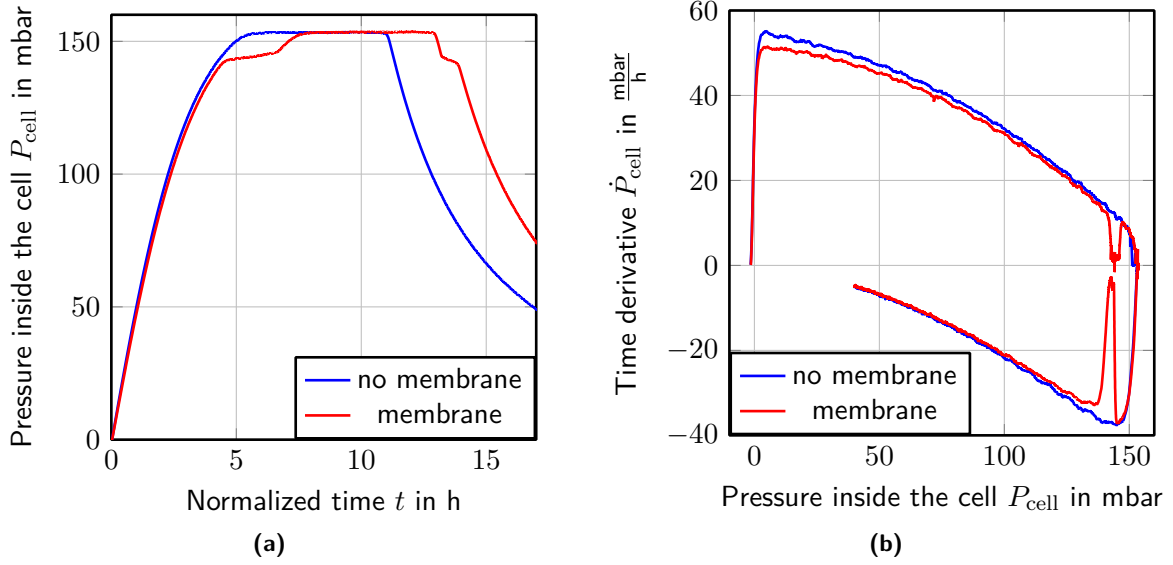


Figure 4.1 Raw volumetric isotherm data recorded with the experimental setup as explained in ?? for one cycle without a membrane inside the cell and one with a membrane inside the cell. (a) shows the pressure values over time making the condensation and evaporation plateaus of absorption and desorption of hexane within the membrane's pores visible. (b) is the pressure loop which is relevant for the computation of the isotherms. Again, the before mentioned plateaus are visible as dips in the time derivative of the pressure.

As the temperature of the system is regulated ($T = T_1 = T_2 = \text{const.}$) and because $V = V_1 \approx V_2$ since $V_{\text{mem}} \ll V_1$, equation eq. (4.1) yields

$$n_2^{\text{membrane}} = \frac{V}{RT} \int_0^{t_2} (\dot{P}_1(t'_1) - \dot{P}_2(t'_2)) dt'_2. \quad (4.2)$$

Important at this point is the dependency of $\dot{P}_1(t_1)$ on t_1 while the integration is over t_2 .

As the experimental setup yields discreet values at given time intervals Δt , the data evaluation makes use of a sum rather than an integration.

$$n = \frac{V}{RT} \sum (\dot{P}_1(P_1 = P_2) - \dot{P}_2(P_2)) \cdot \Delta t \quad (4.3)$$

yields the molar amount of hexane condensed inside the membrane. Figure fig. 4.2(b) shows the result of the integration eq. (4.3) for membrane 296d. It is a absorption and desorption isotherm for hexane inside the porous alumina membrane. The bulk condensation and evaporation is not visible, as it is also recorded with the reference isotherm without membrane inside the cell.

What stings the eye is that the sharp rise of the condensation branch does not start at the liquid fraction $LF = 0$. The same goes for the evaporation branch. It only drops to a liquid fraction value $LF > 0$ and then decreases superimposed with the condensation branch. While it would be reasonable to renormalize the graph so only the mentioned sharp rise and drop are relevant for the isotherm as this part is where the pores fill or empty at spinodal or equilibrium pressure (??), it is not done here. The reason for this is that the initial rise of the isotherms is assumed to be due to the build up of a film on the membranes surfaces. This is part of the theory of condensation and evaporation in confinement even though the film is ignored in the basic KELVIN equation (??). ???MAKE A COMPUTATION AS TO HOW MANY MOLES OF LIQUID ARE EXPECTED FOR THE FILMS ON ONE SINGLE MEMBRANE???

Moreover, the plots

$$i \text{ over } j, \quad i \in \{n, LF, FF\}, \quad j \in \{P_{\text{cell}}, P_{\text{rel}}, D_{\text{kelvin}}\} \quad (4.4)$$

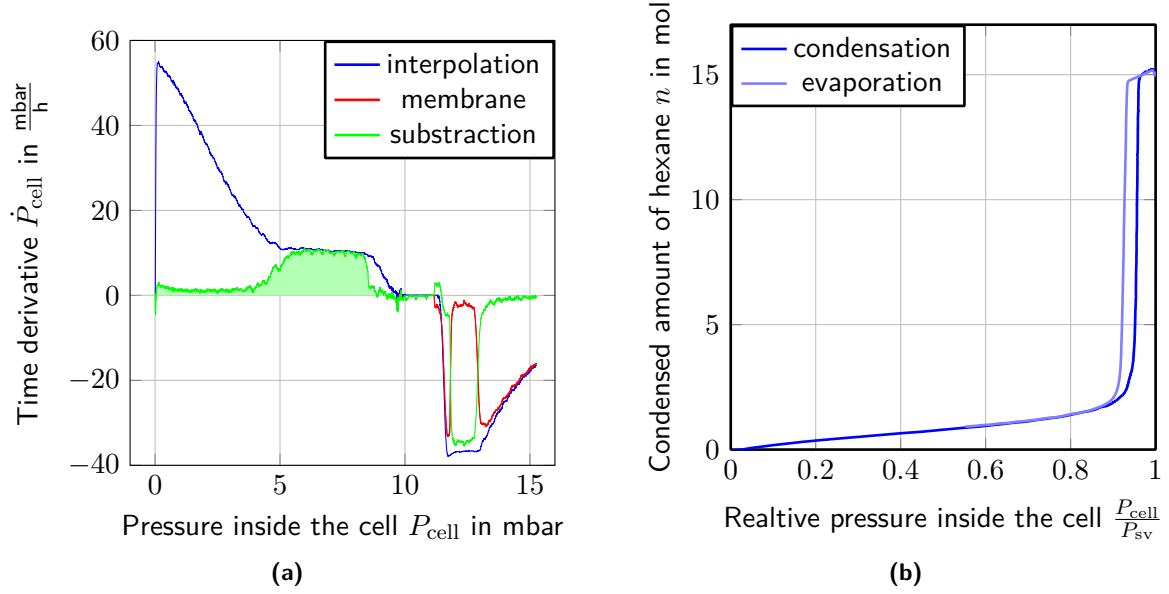


Figure 4.2 (a) shows the raw data of the isotherm with membrane and interpolation of the reference isotherm without membrane. Also, the subtraction of the latter (compare integrand of eq. (4.1)) is plotted where the area to be integrated for the absorption and desorption isotherm is shaded light green. The integration according to eq. (4.3) results in the isotherm displayed in (b).

are of interest, where

$$P_{\text{rel}} = \frac{P_{\text{cell}}}{P_{\text{sv}}^{\text{exp}}}, \quad (4.5)$$

with the saturated vapor pressure P_{sv} .

$$LF = \frac{n}{n_{\text{max}}} \quad (4.6)$$

is the liquid fraction of hexane condensed inside the pores of the membrane using the total maximum amount of condensed hexane n_{max} and last,

$$FF = \frac{V_{\text{hex}}^{\text{cond}}}{V_{\text{mem}}} \quad (4.7)$$

with the volume of condensed hexane $V_{\text{hex}}^{\text{cond}}$ and the membrane's volume V_{mem} , is the filled fraction of the membrane. Its maximum corresponds to the porosity of the membrane. For the computation please refer to ??.

For the computation of the introduced physical sizes, the saturated vapor pressure P_{sv} must be determined.

4.1.1.1 Porosity

Equation eq. (4.3) gives the molar amount of hexane n_{hex} condensed inside the membrane's pores. Furthermore, for the given pressures 0 mbar to 160 mbar hexane in its liquid form can be regarded as incompressible and therefore the hexane's volume be computed via

$$V_{\text{hex}} = n_{\text{hex}} \cdot V_{\text{mol,hex}}.$$

. The thickness l_{pore} of the membrane is easily determinable via MEB views since its magnitude is micrometers. Finally, the area A_{mem} of the measured samples is derived from a photo taken using binoculars.

Using these information the porosity ϕ of a given membrane is given by

$$\phi = 1 - \frac{V_{\text{hex}}}{V_{\text{mem}}}, \quad (4.8)$$

with the membrane's volume

$$V_{\text{mem}} = A_{\text{mem}} \cdot l_{\text{pore}}.$$

4.1.1.2 Determination of the saturated vapor pressure

As the bulk condensation plateau shows a slight drift (compare figure fig. 4.1), using the maximum measured pressure P_{cell} does not yield the saturated vapor pressure P_{sv} but a higher value. In addition, depending on the contamination of the system by air or degassing grease, the measured value for P_{sv} shifts due to the partial pressures. To probe the reproducibility of an isotherm loop including the grade of contamination, the node[anchor=south]maximum measured pressure for different membranes is compared. As the system is opened to replace the membrane in between the isotherms, each cycle is independent. For the change of membrane process please read ???. The result of the experiment is that $P_{\text{sv}}^{\text{exp}}$ fluctuates by

$$\delta P_{\text{sv}}^{\text{exp}} = \pm 0,5 \text{ mbar}. \quad (4.9)$$

As the relevant plateau of condensation and evaporation inside the pores of the membrane occur at about

$$P_{\text{plateaus}} = 140 \text{ mbar}, \quad (4.10)$$

$\delta P_{\text{sv}}^{\text{exp}}$ translates to an error of about

$$\delta P_{\text{rel}} \leq \pm 0,005. \quad (4.11)$$

4.1.1.3 Diameter error using Kelvin equation

GAUSSIAN error propagation to check the precision of the experiment.

4.1.2 Optical measurements

As mentioned in ??, the light transmission setup is independent from the volumetric measurements and also the evaluations do not depend on each other. The light transmission is rather a tool to check on the theory of evaporation and condensation within the membrane using a different approach.

To compute the transmission coefficient of a membrane, it is measured in dry state using the same transmission setup as during the volumetric experiment yielding $T_{\text{mem}}^{\text{dry}}$. Then, the first measured intensity value I_0 of a given isotherm is assigned to the dry coefficient as at this point no hexane is condensed inside of the membranes pores yet. From there on, each intensity measurement is translated to a transmission coefficient according to

$$T(t) = T_{\text{mem}}^{\text{dry}} \cdot \frac{I_0}{I(t)}. \quad (4.12)$$

The aquired physical size can be interpreted as explained in the following ??.

As a forword shall be mentioned that the observed transmission drops' magnitude cannot be explained by simple media transmissions as explained in ??. Even counting multiple transitions for a diagonal transmission of a membrane, the regular transmission is not a sufficient explanation as the filled state of a membrane should by that theory be less transmitting than the empty state whereas the opposite is observed. To explain the phenomena, RAYLEIGH scattering and index matching, which are explained in ?? and ?? respectively, must be taken into account.

4.2 Conducted measurements

General: From one wafer we can test different things as we have 12 membranes. Wafer produced as a whole so membranes should be equivalent. ADD THE CIRCLE HERE!!!

Membranes of four different wafers produced according to ?? have been measured. The wafers specifications are noted in table 4.1. For the wafers 295 and 296, the membranes' names correspond to certain positions of the wafer as shown in ???.

Table 4.1 Wafer specifications. The wafers thickness l_{pore} , floating time t_{float} of the *barrier layer* dissolution process and pore diameter dispersion $\Delta d_{\text{pore}}^{\text{MEB}}$ measured by electron beam microscopy are noted. The latter two parameters apply to the open pore membranes of the respective wafer.

Wafer	l_{pore} [μm]	t_{float} [min]	$\Delta d_{\text{pore}}^{\text{MEB}}$ [nm]
292	60	0	
294	60	0	
295	60	35	
296	30	40	7

4.3 Inhomogeneities on one wafer

4.4 Comparison of closed and open pores

Show comparison of 294, 295 and 296. Speak about the context to theory. Testing the efficiency of opening procedure. Theory test relies on the fact that pores are well open. ADD ONE THAT DID NOT WORK

Hysteresis for closed: corrugations

Hysteresis difference: Coherent with theory

4.4.1 Bad open pores

Talks about 294 and leads to

4.4.2 Inverse funnelling

4.4.2.1 Immersion experiment

Derive and explain etch rate gradient and influence on the pores' shape.

4.4.2.2 Inverse funnelling upon barrier layer dissolution

Explain that the pores appear to be straightened bc of floating. Refer to the theory, that there are two sorts of alumina (pure and acid polluted).

4.4.3 Etch rate difference

Introduce the conducted experiments shortly.

4.4.3.1 Pore opening widening pores much less than expected

Use the example of 292d to explain that the etch rate along the pore axis must be different from the radial one. Conclusion: etch rate offset!S

4.4.3.2 Floating experiment

Explain that the shapes of the isotherms are correct, but that no real conclusion could be made due to the bad MEB views.

4.4.4 Do thinner membranes improve things?

Compare 295 and 296. Talk about the sharpness of both, the volumetric and the optical isotherm. Also speak about the rather broad isotherm for closed pores of 295 which is not understood. Use diameter translation by Kelvin law!!

4.5 Testing theory using electron beam microscopy

4.6 Pore size reduction using atomic layer deposition

4.7 Isotherms proves powerful to detect and characterize defects

Bring up membrane 293 (constricted pore ends) and membrane 295c (closed pores).

Bibliography

[Cd15] Universität Konstanz: Corporate Design Manual. Universität Konstanz, (2015)